Flow, Turbulence and Combustion (2024) 113:1145–1160
https://doi.org/10.1007/s10494-024-00560-4

RESEARCH

A Comparison of Evaluation Methodologies of the Fractal Dimension of Premixed Turbulent Flames in 2D and 3D Using Direct Numerical Simulation Data

Marco Herbert[1] · **Nilanjan Chakraborty**[2] · **Markus Klein**[1]

Received: 18 April 2024 / Accepted: 7 June 2024 / Published online: 17 July 2024

Abstract
A Direct Numerical Simulation (DNS) database of statistically planar flames ranging from the wrinkled flamelets to the thin reaction zones regime and DNS data for a Bunsen premixed flame representing the wrinkled flamelets regime have been utilised to evaluate the fractal dimensions of flame surfaces using the filtering dimension method, the box-counting algorithm and the correlation dimension approach. The fractal dimension evaluated based on the fully resolved three-dimensional data has been found to be reasonably approximated by adding unity to the equivalent fractal dimension evaluated based on two-dimensional projections irrespective of the methodology of extracting fractal dimension. This indicates that the flame surface can be approximated as a self-similar fractal surface for the range of Karlovitz and Damköhler numbers considered here. While all methods, provide results identical to each other for benchmark problems, it has been found that the fractal dimension evaluation based on box-counting method provides almost identical results as that obtained using the filtering dimension method for both three and two dimensions, while the fractal dimensions based on the correlation dimension tend to be slightly smaller. The findings of the current analysis have the potential to be used to reliably estimate the actual fractal dimension in 3D based on experimentally obtained 2D binarised reaction progress variable field. The inner cut-off scales estimated based on all three methodologies yield comparable results in terms of order of magnitude with the box-counting method predicting a smaller value of inner cut-off scale in comparison to other methods. The execution times for fractal dimension extraction based on filtering dimension and box-counting methodologies are found to be comparable but the correlation dimension method is found to be considerably faster than the two alternative approaches and provides results consistent with theoretical bounds in all cases.

Keywords Fractal dimension · Filtering dimension · Box-counting · Correlation dimension · Premixed turbulent flames · Direct Numerical Simulations

✉ Markus Klein
markus.klein@unibw.de

[1] Department of Aerospace Engineering, Bundeswehr University Munich, LRT1, Werner-Heisenberg-Weg 39, 85577 Neubiberg, Germany

[2] School of Engineering, Newcastle University, Claremont Road, Newcastle-Upon-Tyne NE1 7RU, UK

1 Introduction

The flame surface area in turbulent premixed flames is a quantity of fundamental interest from the point of view of parameterising the burning rate (Damköhler 1940; Bray 1990; Driscoll 2008; Wabel et al. 2017; Chakraborty et al. 2019; Ahmed et al. 2021) and modelling (Bray and Peters 1990; Pope 1988; Candel and Poinsot 1990; Peters 2000; Kerstein 1988; Gouldin et al. 1989; Gülder and Smallwood 1995; North and Santavicca 1990; Smallwood et al. 1995; Yoshiyama et al. 2001; Charlette et al. 2002; Fureby 2005; Cohe et al. 2007; Cintosun et al. 2007; Chakraborty and Klein 2008; Keppeler et al. 2012; Chatakonda 2012; Chatakonda et al. 2013) of premixed turbulent combustion. The flame surface is often modelled based on fractal theory (Kerstein 1988; Gouldin et al. 1989; Gülder and Smallwood 1995; North and Santavicca 1990; Smallwood et al. 1995; Yoshiyama et al. 2001; Charlette et al. 2002; Fureby 2005; Cohe et al. 2007; Cintosun et al. 2007; Chakraborty and Klein 2008; Keppeler et al. 2012; Chatakonda 2012; Chatakonda et al. 2013), where the flame is assumed to have self-similar properties characteristic for fractals. In the context of the fractal description of the flame, the estimation of fractal dimension D_F plays a key role in the evaluation of flame surface area and modelling of the Flame Surface Density (Kerstein 1988; Gouldin et al. 1989; Gülder and Smallwood 1995; North and Santavicca 1990; Smallwood et al. 1995; Yoshiyama et al. 2001; Charlette et al. 2002; Fureby 2005; Cohe et al. 2007; Cintosun et al. 2007; Chakraborty and Klein 2008; Keppeler et al. 2012; Chatakonda 2012; Chatakonda et al. 2013). In experimental analyses, the fractal dimension of the premixed flame surface is often evaluated based on 2D flame surface visualisations (i.e., henceforth D_{2F} refers to the fractal dimension evaluated based on 2D contours) and the actual fractal dimension in 3D (i.e., D_{3F}) can be obtained by Mandelbrot's additive rule: $D_{3F} = D_{2F} + 1.0$ (Mandelbrot 1983) based on the assumption of isotropic self-similarity of the fractal surface. This methodology was widely used in several experimental analyses (Gülder and Smallwood 1995; North and Santavicca 1990; Smallwood et al. 1995; Yoshiyama et al. 2001; Cohe et al. 2007; Cintosun et al. 2007). However, the assessment of the validity of the assumption behind Mandelbrot's additive rule (Mandelbrot 1983) by experimental means remains a prohibitively challenging task. Chatakonda et al. (2013) assessed the additive rule of Mandelbrot (1983) based on the box-counting method using Direct Numerical Simulation (DNS) data for low Damköhler number conventional and thermonuclear flames. However, the influence of thermal expansion remains strong for premixed flames with high (low) Damköhler (Karlovitz) numbers (Chakraborty 2021) and this influence is predominantly felt in the local flame normal direction. Thus, the effect of anisotropy is expected to be strong for high (low) Damköhler (Karlovitz) number conditions. Thus, it is worthwhile to assess if Mandelbrot's additive rule remains valid even for high values of Damköhler number where the anisotropic effects are expected to be strong. Moreover, the analysis by Chatakonda et al. (2013) employed the box-counting technique to assess the applicability of Mandelbrot's additive rule (Mandelbrot 1983) for turbulent premixed flames. However, the fractal dimension can be evaluated using various methodologies. Previous analyses (Wang et al. 2022) on complex systems revealed that there can be differences between the fractal dimensions evaluated using box-counting and filtering dimension schemes (i.e., henceforth between D^{BC} and D^{FD}). The fractal dimension is also closely related to the correlation dimension (henceforth denoted D^{CD}) which is much easier to compute (Grassberger and Procaccia 1983). According to the best of authors knowledge, the correlation dimension method has not been applied to the analysis of turbulent flames so far.

Thus, it is important to assess whether the evaluation methodology affects the value of the fractal dimension of the flame surface and the applicability of Mandelbrot's additive rule.

In this analysis, 3D DNS data of statistically planar and Bunsen flames has been considered to evaluate the relation between fractal dimensions based on 2D projections and actual 3D flame surfaces based on box-counting (BC), filtering dimension (FD) and correlation dimension (CD) methodologies. Moreover, the sensitivity of the obtained fractal dimension on the evaluation methodology has also been analysed based on these DNS databases. The main objectives of the current analysis are: (a) to assess whether Mandelbrot's additive rule (i.e., $D_{3F} = D_{2F} + 1.0$) is valid for a wide range of values of Damköhler and Karlovitz numbers; (b) to demonstrate the sensitivity of the evaluation methodology of the fractal dimension and the validity of Mandelbrot's additive rule using a DNS database for statistically planar and Bunsen premixed flames.

2 Mathematical Background

The ratio of the turbulent flame surface area A_T to the area related to the mean flame brush A_L can be expressed using the FD in the following manner (Kerstein 1988; Gouldin et al. 1989; Gülder and Smallwood 1995; North and Santavicca 1990; Smallwood et al. 1995; Yoshiyama et al. 2001; Charlette et al. 2002; Fureby 2005; Cohe et al. 2007; Cintosun et al. 2007; Chakraborty and Klein 2008; Keppeler et al. 2012; Chatakonda 2012; Chatakonda et al. 2013):

$$A_T/A_L = \left(\epsilon_0/\epsilon_i\right)^{n_p} \tag{1}$$

where ϵ_i and ϵ_o are the inner cut-off scale and outer cut-off scale, respectively and n_p is the index associated with filtering dimension. In the context of Large Eddy Simulations (LES) of premixed turbulent flames, the flame surface area A_T is evaluated as (Chakraborty et al. 2019; Ahmed et al. 2021; Chakraborty and Klein 2008; Keppeler et al. 2012; Klein et al. 2020): $A_T = \int_V |\nabla c| dV = \int_V \Sigma_{gen} dV = \langle \Sigma_{gen} \rangle_V$ (here $\langle Q \rangle_V$ is defined as $\langle Q \rangle_V = \int_V Q dV$), where $\Sigma_{gen} = \overline{|\nabla c|}$ is the generalised Flame Surface Density (FSD) with the overbar suggesting a filtering operation in the context of Large Eddy Simulations (LES) where $\overline{Q} = \int Q(\boldsymbol{x} - \boldsymbol{r}) G(\boldsymbol{r}) d\boldsymbol{r}$ is the filtered value of a general variable Q with $G(\boldsymbol{r})$ being the filter function (Boger et al. 1998), which is taken to be a Gaussian filter in this analysis. In the context of LES, the filter width Δ is the outer cut-off scale and the quantity A_L can be estimated as (Chakraborty and Klein 2008; Keppeler et al. 2012; Klein et al. 2020): $A_L = \int_V |\nabla \overline{c}| dV = \langle |\nabla \overline{c}| \rangle_V$. This leads to the following expression (Chakraborty et al. 2019; Ahmed et al. 2021; Chakraborty and Klein 2008):

$$\log\left(\langle \Sigma_{gen} \rangle_V / \langle |\nabla \overline{c}| \rangle_V \right) = n_p \log(\Delta) - n_p \log(\epsilon_i) \tag{2}$$

A linear relation between $\log(\langle \Sigma_{gen} \rangle_V / \langle \nabla \overline{c} | \rangle_V)$ and $\log(\Delta)$ is indicative of the validity of the FD expression and the slope of this linear variation yields n_p. It has been demonstrated in several previous studies (Chakraborty et al. 2019; Ahmed et al. 2021; Chakraborty and Klein 2008) that a linear relation can indeed be obtained between $\log(\langle \Sigma_{gen} \rangle_V / \langle |\nabla \overline{c}| \rangle_V)$ and $\log(\Delta)$ for premixed flames when the filter width is much greater than the flame thickness but smaller than the largest flame wrinkles. The same qualitative behaviour has

been observed in this analysis (shown later in this paper) and thus, Eq. (2) is used for the estimation of D_F^{FD}. In 3D, the fractal dimension based on the FD methodology D_{3F}^{FD} is evaluated as: $D_{3F}^{FD} = n_p + 2$ (Chakraborty et al. 2019; Ahmed et al. 2021; Chakraborty and Klein 2008). For the purpose of extracting the fractal dimension in 2D using the FD method, Σ_{gen} and $|\nabla\overline{c}|$ in Eq. (2) should be replaced by $\Sigma_{2D} = \overline{[(\partial c/\partial x)^2 + (\partial c/\partial y)^2]^{\frac{1}{2}}}^{2D}$ and $|\nabla\overline{c}^{2D}| = (\partial\overline{c}^{2D}/\partial x)^2 + (\partial\overline{c}^{2D}/\partial y)^2]^{1/2}$ where $\overline{Q}^{2D}$ is the 2D filtered value of a general variable Q based on the measurement (i.e., $x-y$) plane. The equivalent FD based fractal dimension of the flame contours in 2D is given by: $D_{2F}^{FD} = n_p + 1$.

The BC method is one of the most popular approximate methods for estimating the fractal dimension of a surface irrespective of whether it shows self-similarity or not. The BC algorithm is split into three major steps:

- The first step involves creating a grid with the same number of unit boxes n in each direction (x, y, and z for 3D; and in one direction less for 2D). This yields several voxels or pixels (for 3D or 2D) of the processed object, which is the power of 3 or 2. This process is done in such a manner that no voxels/pixels are wasted (Wang et al. 2022).
- The second part involves placing the surface in the grid and varying n by a chosen scaling factor ϵ until a limiting dimension is reached. This limiting dimension is often governed by the resolution of the experimental/computational data in the cases considered. The scaling factor is chosen such that $1/\epsilon \sim \Delta$.
- The last part is to obtain a dynamic relationship between the number of boxes occupied by the surface $N(\epsilon)$ and the scaling factor ϵ.

The resulting fractal dimension based on the BC method is given by (Chatakonda 2012; Chatakonda et al. 2013; Mandelbrot 1983; Wang et al. 2022; Buczkowski et al. 1998):

$$D_F^{BC} = lim_{\epsilon\to 0}\log(N(\epsilon))/\log(1/\epsilon) \tag{3}$$

Equation (3) is the standard definition for the fractal dimension in the BC methodology, which provides the slope of the linear part of the variation of $\log(N(\epsilon))$ and $\log(1/\epsilon)$ in the limit of vanishing ϵ (Buczkowski et al. 1998). For any numerical data the dynamic range is limited and therefore in all practical applications of the BC methodology the slope is approximated by a linear regression.

The CD method has been introduced by Grassberger and Procaccia (1983) as a characteristic measure of strange attractors. It measures the closeness of points in space by employing the sum:

$$C(\Delta) = lim_{N\to\infty}\frac{1}{N(N-1)}\sum_{i=1}^{N}\sum_{j=i+1}^{N}\Theta(\Delta - ||x_i - x_j||) \tag{4}$$

Here N describes the number of points on the surface for which the correlation dimension is evaluated. The correlation sum can be approximated by choosing a sample of random points on the object. Here, Θ is the Heaviside function of the scale Δ and the distance between two points, $C(\Delta)$ is the normalised sum of all points within distance Δ of each other. The resulting fractal dimension can be obtained by assuming a power law relation between $C(\Delta)$ and Δ (Grassberger and Procaccia 1983).

$$C(\Delta) = \Delta^{D_F^{CD}} \tag{5}$$

The FD, BC and CD algorithms used in the present analysis have been validated using fractals with a known Hausdorff dimension (D_F^{Ha}). In order to apply the FD method the fractal surface has to be converted to a binarised image (e.g. for a flame burned and unburned areas) which is subsequently filtered with a very narrow Gaussian filter in order to avoid ill-conditioned numerical differentiation in the FD method. In contrast the BC and CD method are based on a well-defined surface with a thickness of one pixel. The validation of the methodologies considered here (i.e., FD, BC and CD methodologies) is provided in the Appendix. The validated algorithms have been applied to the flame surfaces of the DNS data in Sect. 4 of this paper.

3 DNS Database

The present analysis considered three-dimensional DNS databases of statistically planar (Ahmed et al. 2019a, b, 2021) and statistically axisymmetric turbulent premixed Bunsen (Chakraborty et al. 2019; Klein et al. 2018) flames. For both configurations, a single step Arrhenius-type irreversible chemical reaction is considered for the sake of computational economy. The simplification of chemistry does not affect the conclusions related to fractal dimensions. A well-known compressible DNS code SENGA + (Chakraborty et al. 2019; Ahmed et al. 2019a, b, 2021; Klein et al. 2018) has been used for the simulations where all the spatial derivatives are approximated by high-order finite difference schemes (10th order central difference scheme for the internal grid points and the order of accuracy drops to a one-sided 2nd order scheme at non-periodic boundaries) and a low-storage 3rd order Runge–Kutta scheme is used for temporal advancement. The standard Navier–Stokes Characteristic Boundary Conditions (NSCBC) (Poinsot and Lele 1992) have been employed for turbulent inflow and partially non-reflecting outflow boundaries in the direction of mean flame propagation (here taken to be the x-direction) and transverse boundaries (i.e., y and z directions) are considered to be periodic for the statistically planar flame configuration. The mean inlet velocity U_{mean} for this configuration is gradually modified to match the turbulent burning velocity to ensure an eventual statistically stationary state. The domain size for statistically planar turbulent premixed flame simulations is $79.5\delta_{th} \times \left(39.8\delta_{th}\right)^2$, which is discretised by a uniform Cartesian grid of dimension $800 \times 400 \times 400$ where $\delta_{th} = (T_{ad} - T_0)/\max|\nabla T|_L$ is the thermal flame thickness with T, T_0 and T_{ad} being the dimensional temperature, unburned gas temperature and the adiabatic flame temperature, respectively. The root-mean-square turbulent velocity fluctuation normalised by the unstrained laminar burning velocity u'/S_L, integral length scale to thermal flame thickness ratio l/δ_{th} along with the values of Damköhler number $Da = lS_L/u'\delta_{th}$, Karlovitz number $Ka = \left(u'/S_L\right)^{3/2}\left(l/\delta_{th}\right)^{-1/2}$ and heat release parameter $\tau = (T_{ad} - T_0)/T_0$ are summarised in Table 1. A bandwidth-filtered forcing method (Klein et al. 2017) in physical space has been employed for the unburned gas forcing so that the prescribed turbulence intensity u'/S_L and the desired value of l/δ_{th} are maintained. The total simulation time for all statistically planar flame cases remains greater than one through pass time and at least 10 eddy turnover times (i.e., $10l/u'$) to ensure a statistically steady state in all cases. Interested readers are referred to Ahmed et al. (2019b, 2021) and Klein et al. (2018) for further information on this dataset. Instantaneous $c = 0.1$ (yellow) and $c = 0.9$ (red) isosurfaces of reaction progress for the statistically planar flame cases are depicted in Fig. 1a–c, which shows that

Table 1 The attributes of the DNS databases considered for this analysis

Statistically planar flame cases						
Cases	u'/S_L	l/δ_{th}	Da	Ka	τ	
AP	1.0	3.0	3.0	0.58	4.5	Corrugated flamelets
BP	3.0	3.0	1.0	3.0	4.5	Thin reaction zones
CP	5.0	3.0	0.6	6.5	4.5	Thin reaction zones
DP	7.5	3.0	0.4	11.85	4.5	Thin reaction zones
EP	10.0	3.0	0.33	18.3	4.5	Thin reaction zones
Bunsen burner flame						
Case	u'_{inlet}/S_L	l_{inlet}/δ_{th}	Da	Ka	τ	Combustion regime
AB	0.68	7.46	10.94	0.21	6.5	Wrinkled flamelets

The first letter of the case name corresponds to the names used in previous papers (Ahmed et al. 2021, b; Klein et al. 2018) and P and B refer to statistically planar and Bunsen premixed flames, respectively

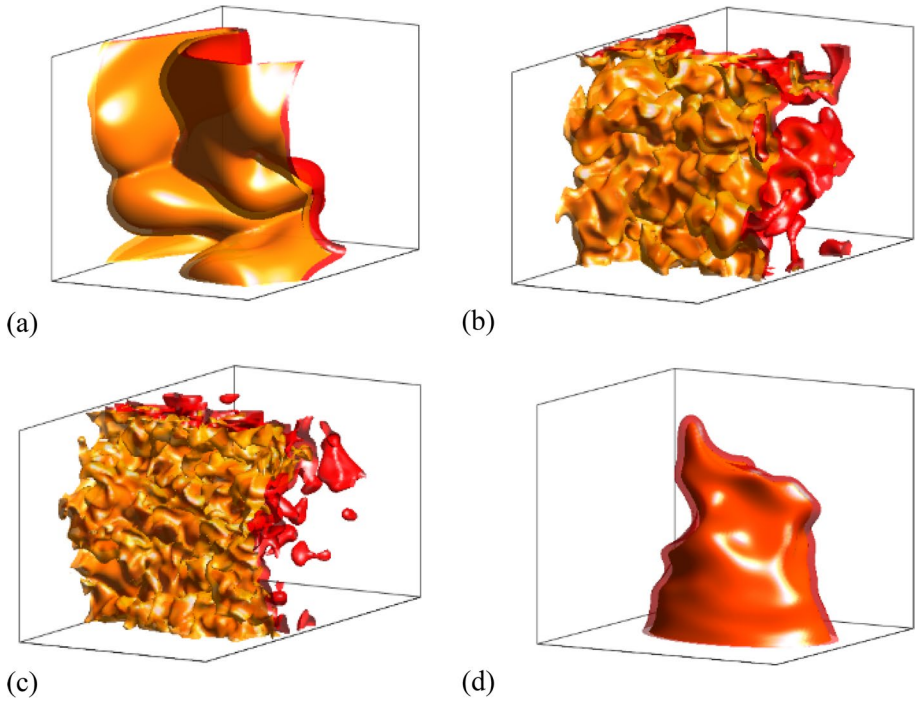

Fig. 1 Instantaneous $c = 0.1$ (yellow) and $c = 0.9$ (red) isosurfaces of reaction progress for (**a–d**) cases AP, CP, EP, AB

the extents of flame wrinkling and flame brush thickening increase with increasing Karlovitz number.

For the Bunsen flame simulations, the axial direction is taken to align with x-direction and all the boundaries apart from the inlet are taken to be partially non-reflecting which is specified using the NSCBC technique (Poinsot and Lele 1992). A hyperbolic tangent-like profile is used for the mean velocity specification at the inlet. Turbulent velocity fluctuations are then superimposed on this mean profile by generating velocity fluctuations using a modified version of the method suggested in Klein et al. (2003), replacing the Gaussian filter with an autoregressive AR1 process in the axial direction. The reacting scalars have been initialised with an unstrained premixed laminar flame solution expressed as a function of the radial distance from the centre of the inlet. The computational domain is taken to be a cube with each side equalling to $2d_n$ where d_n is the diameter of the nozzle, which is discretised using a uniform Cartesian grid of dimension $750 \times 750 \times 750$. For the Bunsen flame configuration, the domain size corresponds to $75\delta_{th} \times 75\delta_{th} \times 75\delta_{th}$ and the normalised mean inflow velocity is $U_B/S_L = 6$. The normalised root-mean-square inlet velocity u'_{inlet}/S_L and normalised integral length scale of turbulence at the inlet (l_{inlet}/δ_{th}) are summarised along with the Damköhler number $Da = lS_L/u'_{inlet}\delta_{th}$, Karlovitz number $Ka = \left(u'_{inlet}/S_L\right)^{1.5}\left(l/\delta_{th}\right)^{-0.5}$ and heat release parameter $\tau = (T_{ad} - T_0)/T_0$ in Table 1.

All statistics presented in this paper for the Bunsen flame correspond to at least two flow-through and two initial eddy turnover times. Instantaneous $c = 0.1$ (yellow) and $c = 0.9$ (red) isosurfaces of reaction progress variable for the DNS data of the Bunsen flame considered here are shown in Fig. 1d. The contours of c in Fig. 1d remain parallel to each other and exhibit large-scale wrinkles due to the background turbulent motion, which is characteristic of the combustion within the wrinkled flamelets regime (Peters 2000).

For both configurations, standard values are taken for Prandtl number (i.e., $Pr = 0.7$), Zel'dovich number (i.e., $\beta = T_{ac}\left(T_{ad} - T_0\right)/T_{ad}^2 = 6.0$ with T_{ac} being the activation temperature) and the ratio of specific heats (i.e., $\gamma = 1.4$).

It is worth noting that all the statistics needed for the current analysis are taken after the simulations have reached a steady state (as specified before). The fractal dimensions of the flame did not change significantly once the steady state has been reached. For the planar flames results have been averaged in two homogeneous directions and for the Bunsen flames in circumferential direction using at least ten different snapshots.

4 Results and Discussion

In order to demonstrate the methodologies of extracting the fractal dimensions, the variation of $\log(\langle\Sigma_{gen}\rangle_V/\langle|\nabla\overline{c}|\rangle_V)$ with $\log(\Delta/\delta_{th})$ for case EP is exemplarily shown in Fig. 2a and the corresponding variation of $\log(\langle\Sigma_{2D}\rangle_V/\langle|\nabla\overline{c}^{2D}|\rangle_V)$ with $\log(\Delta/\delta_{th})$ is shown in Fig. 2b. It can be seen from Fig. 2a and b that a linear relationship is obtained for $\Delta/\delta_{th} > 1.0$ and the slope of the linear part provides the FD exponent n_p in 3D (where $D_{3F}^{FD} = n_p + 2$) and 2D (where $D_{2F}^{FD} = n_p + 1$). Similarly, the slope of the linear part of the variation of $\log(A(\triangle))$ with $\log\left(\triangle/\delta_{th}\right)$ in 3D, A being an area estimate, and $\log(L(\triangle))$ with $\log\left(\triangle/\delta_{th}\right)$ in 2D, L being a length estimate, provide the BC values of fractal dimensions in 3D (i.e., D_{3F}^{BC}) and 2D (i.e., D_{2F}^{BC}), as shown exemplarily in Figs. 2c and 2d, respectively for the $c = 0.8$ isosurface in case EP. Finally, Fig. 2e and f show, variations of $\log(\mathrm{C}(\Delta))$ with $\log(\Delta/\delta_{th})$ with a linear relation at $\Delta/\delta_{th} > 1.0$ resulting in the CD values for the fractal dimension.

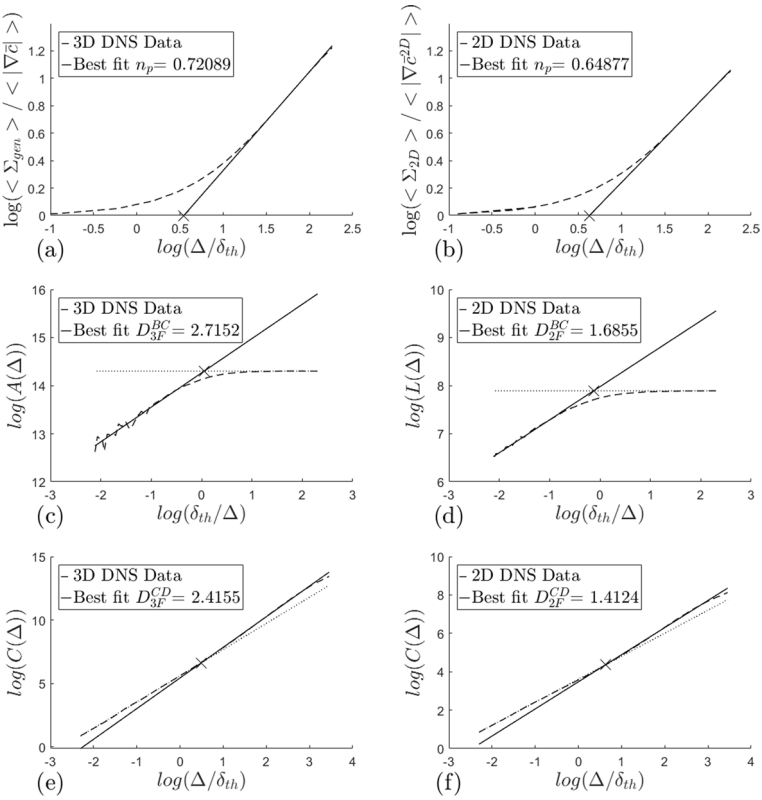

Fig. 2 Variations of **a** $\log(\langle\Sigma_{gen}\rangle_V/\langle|\nabla\tilde{c}|\rangle_V)$ with $\log(\Delta/\delta_{th})$ in 3D, **b** $\log(\langle\Sigma_{2D}\rangle_V/\langle|\nabla\tilde{c}^{2D}|\rangle_V)$ with $\log(\Delta/\delta_{th})$ in 2D, **c** $\log(A(\Delta))$ with $\log(\Delta/\delta_{th})$ in 3D, A being an area estimate, **d** $\log(L(\Delta))$ with $\log(\Delta/\delta_{th})$ in 2D, L being a length estimate, **e** $\log(C(\Delta))$ with $\log(\Delta/\delta_{th})$ in 3D, **f** $\log(C(\Delta))$ with $\log(\Delta/\delta_{th})$ in 2D. The x-coordinate of the crosses at the intersection point of the solid line with the x-axis (dotted line) in subfigures **a** and **b** (subfigures (**c**–**f**)) provides the inner cut-off scale. Box-counting and correlation dimension results in Figs. 2, 3 and 5 correspond to the $c = 0.8$ isosurface

The values of fractal dimension based on 2D reaction progress variable fields using FD, BC and CD methodologies (i.e., D_{2F}^{FD}, D_{2F}^{BC} and D_{2F}^{CD}) for the DNS cases of statistically planar and Bunsen flames are shown in Fig. 3. It can be seen from Fig. 3 that D_{2F}^{BC} assumes almost identical values as D_{2F}^{FD} for both flame configurations, while D_{2F}^{CD} attains slightly smaller values especially for high turbulence intensities. The corresponding fractal dimensions based on three-dimensional data using BC, FD and CD methodologies (i.e., D_{3F}^{FD}, D_{3F}^{BC} and D_{3F}^{CD}) for the DNS data are also shown in Fig. 3. It can be seen that $D_{3F}^{FD} \approx D_{3F}^{BC} \approx D_{3F}^{CD}$ is obtained for all the DNS cases considered here with the FD method yielding consistently the largest and the CD method the smallest values of fractal dimension. It is to be noted that Cintosun et al. (2007) employed different methodologies to estimate the fractal dimension of the flame surface based on 2D experimental measurements and they yielded

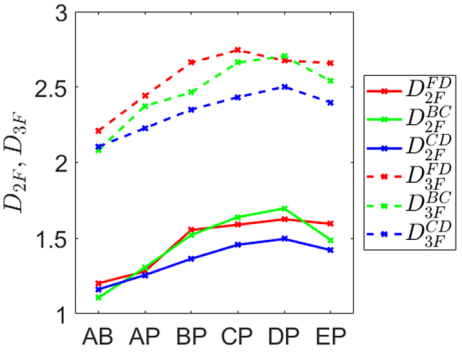

Fig. 3 Dashed lines: Fractal ... Fractal dimension based on two-dimensional contours using filtering dimension box-counting and correlation dimension methodologies (i.e., D_{2F}^{FD}, D_{2F}^{BC} and D_{2F}^{CD}) for DNS cases of statistically planar and Bunsen burner flames; solid lines: fractal ...dimensions based on three-dimensional data using BC, filtering dimension and correlation dimension methodologies (i.e., D_{3F}^{FD}, D_{3F}^{BC} and D_{3F}^{CD})

comparable values. Moreover, Chatakonda (2012) reported good agreement between fractal dimensions extracted from box-counting and filtering dimension methodologies based on DNS data for $Ka \gg 1$ flames.

It can further be seen from Fig. 3 that D_{3F}^{FD}, D_{3F}^{BC} and D_{3F}^{CD} remain close to $8/3$ for the statistically planar flame with $Ka \gg 1$ (e.g. cases CP, DP and EP) which is consistent with the expectation that the premixed flame surfaces exhibit fractal dimension corresponding to passive scalar isosurfaces for $Ka \gg 1.0$) (Ahmed et al. 2021; Chatakonda 2012; Chatakonda et al. 2013). A drop in fractal dimension in case EP in comparison to case DP is a consequence of a smaller value of A_T/A_L in case EP, which was demonstrated elsewhere (Varma et al. 2021). The extent of a flame–flame interaction and the smoothing of highly curved surfaces as a result of molecular diffusion process (Yu and Lipatnikov 2017) strengthens for $Ka \gg 1$ which, influences both dilatation rate and flame displacement speed statistics in such a manner that the flame surface area may decrease with an increase in u'/S_L. Moreover, Denet (1999) demonstrated the possibility of a drop in turbulent burning velocity with an increase in turbulence intensity based on analytical means. The possible decrease of burning velocity beyond a maximum value has also been reported by Driscoll (2008) and it was explained in terms of the loss of flame surface area due to flame surface merging and quenching at large turbulence intensities.

It is noted that values slightly larger than $8/3$ have been found using the FD and BC method. It can be appreciated from Eqs. (2) and (3) that D_{3F}^{FD} and D_{2F}^{FD} are evaluated based

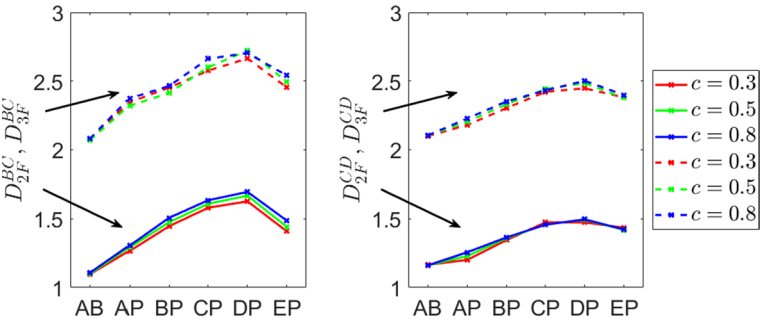

Fig. 4 (left) Variations of D_{2F}^{BC} and D_{3F}^{BC} for $c = 0.3, 0.5$ and 0.8 isosurfaces for cases AP, BP, CP, DP, EP and AB; (right) Variations of D_{2F}^{CD} and D_{3F}^{CD} for $c = 0.3, 0.5$ and 0.8 isosurfaces for cases AP, BP, CP, DP, EP and AB

on volume-integrated quantities. In contrast the fractal dimensions based on the BC and CD method (i.e., D_{2F}^{BC}, D_{3F}^{BC}, D_{2F}^{CD} and D_{3F}^{CD}) depend on the choice of the c isosurface.

In Fig. 3, the BC results based on $c = 0.8$ isosurface are presented because the maximum values of reaction rate and chemical heat release for the unstretched laminar premixed flame corresponding to the current thermochemistry occur close to $c = 0.8$. However, the sensitivity of the choice of the reaction progress variable c isosurface on D_{2F}^{BC} and D_{3F}^{BC} is demonstrated in Fig. 4, which shows that the choice of the c isosurface does not affect the numerical values of D_{2F}^{BC} and D_{3F}^{BC} for flames with $Ka < 1$ (i.e., the flames in the wrinkled flamelets/corrugated flamelets regime) but marginally smaller values of fractal dimensions are obtained for smaller values of c (i.e., towards the preheat zone) for the flames in the thin reaction zones regime (i.e., $Ka > 1$). Similarly, Fig. 4 shows the same analysis for D_{2F}^{CD} and D_{3F}^{CD} with results comparable to D_{2F}^{BC} and D_{3F}^{BC}, respectively. As the fractal dimensions estimated by BC and CD are not severely affected by the choice of the c isosurface, the fractal dimensions for BC and CD methodologies will henceforth be associated with the $c = 0.8$ isosurface for the following discussion.

The values of D_{3F}^{FD}, D_{3F}^{BC} and D_{3F}^{CD} are compared to $(D_{2F}^{FD} + 1)$, $(D_{2F}^{BC} + 1)$ and $(D_{2F}^{CD} + 1)$ in Fig. 5 for the DNS cases considered here. Figure 5 shows that $D_{3F}^{FD} = (D_{2F}^{FD} + 1)$, $D_{3F}^{BC} = (D_{2F}^{BC} + 1)$ and $D_{3F}^{CD} = (D_{2F}^{CD} + 1)$ hold reasonably well for all the flames considered here with slightly larger deviations for the FD method. This is found to be consistent with previous findings by Chatakonda et al. (2013), who also reported that $D_{3F}^{BC} = (D_{2F}^{BC} + 1)$ holds mostly for $Da < 1$ flames but the current findings suggest the Mandelbrot's additive rule (Mandelbrot 1983) remains valid for a wide range of values of Da and Ka irrespective of the evaluation methodology of the fractal dimension. This reveals that the small-scale wrinkles of the flame surface exhibit an approximate isotropic self-similar fractal behaviour, which suggests that the fractal dimension estimated based on 2D experimental images (i.e., D_{2F}) can be used to estimate the actual fractal dimension of the flame surface in 3D (i.e., D_{3F}) using $D_{3F} = (D_{2F} + 1)$ for the range of Ka considered here.

In the case of sufficiently large separation between the flame geometry (i.e., mean curvature) and the flame thickness (which should be the case for real flames), the fractal dimension is expected to be independent of the flame geometry. The present results for $Ka \gg 1$ flames considered here are qualitatively consistent with the findings by Chatakonda et al. (2013) for temporally evolving jets. Moreover, the fractal dimensions obtained in this analysis are consistent with literature in the sense that in the flamelet regime Kerstein (1988) suggests a fractal dimension of 7/3, while the maximum fractal

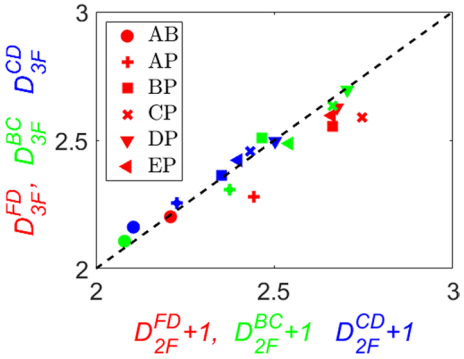

Fig. 5 Variations of D_{3F}^{FD} versus $(D_{2F}^{FD} + 1)$, D_{3F}^{BC} $(D_{2F}^{BC} + 1)$ and D_{3F}^{CD} and $(D_{2F}^{CD} + 1)$ for cases AP, BP, CP, DP, EP and AB

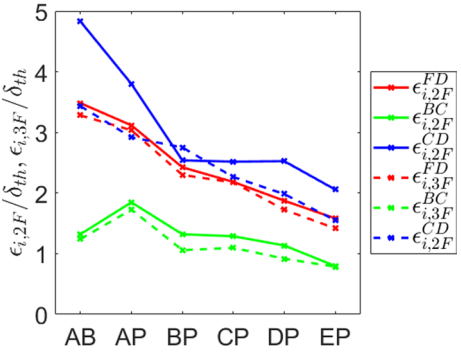

Fig. 6 Solid lines: Inner cut-off scales normalised by δ_{th} based on two-dimensional contours using filtering dimension, box-counting and correlation dimension methodologies (i.e., $\epsilon_{i,2F}^{FD}$, $\epsilon_{i,2F}^{BC}$ and $\epsilon_{i,2F}^{CD}$) for DNS cases of statistically planar and Bunsen burner flames; Dashed lines: Inner cut-off scales based on three-dimensional data using BC, filtering dimension and correlation dimension methodologies (i.e., $\epsilon_{i,3F}^{FD}$, $\epsilon_{i,3F}^{BC}$ and $\epsilon_{i,3F}^{CD}$)

dimension for a flame in the well-mixed regime, as well as a passive scalar isosurface, has been found to be 8/3 (Chatakonda 2012; Chatakonda et al. 2013). Furthermore, the fractal dimensions obtained for the flames considered here are in qualitative agreement with previous DNS results based on high pressure Bunsen flames including non-unity Lewis number effects (Rasool et al. 2020, 2021) and planar flames with shock interaction (Bambauer et al. 2023).

All three methodologies of evaluating the fractal behaviour of flames surfaces are based on considerably different algorithms and different type of data. Hence, it is necessary to critically contrast all approaches with respect to their application to flame surfaces. While the BC and CD method assume an infinitely thin surface (numerically or experimentally resolved with one pixel), the FD method can be directly applied to simulation data characterised by a finite thickness flame front. This implies that the application of the BC and CD methods always requires a pre-processing step for edge detection (Chaib et al. 2023), that can be intricate in itself and involves the selection of a particular isosurface. This potentially makes the results ambiguous for large values of Karlovitz numbers, when turbulent eddies penetrate in the preheat zone or even reaction layer and distort the flame structure. The FD method may not have this problem as it is based on volume averages of the generalised FSD and it can be directly applied to simulation data, whereas, when applied to experimental data, it also requires a binarisation of the image. The FD method is based on filtering the data with a series of increasingly larger filter widths, which results in an increasing flame brush thickness until flame self-interactions become unavoidable. This can sometimes result in a degradation of accuracy because the flame wrinkles cannot be described by a self-similar FD in the case of several flame surface self-intersections. Thus, FD can yield a significant overestimation of D_F in the case of excessive flame self-interactions and can potentially lead to unrealistic values of D_F (e.g., $D_F > 3.0$) (Bambauer et al. 2023). For all methods, the fractal dimension is determined by the slope of a linear function fitted to the linear part of the resulting functional dependence between $\log(\langle\Sigma_{gen}\rangle_V/\langle|\nabla\overline{c}|\rangle_V)$ with $\log(\Delta/\delta_{th})$, $\log(A(\Delta))$ with $\log(\Delta/\delta_{th})$ (or $\log(L(\Delta))$ with $\log(\Delta/\delta_{th})$ in 2D), or $\log(C(\Delta))$ with $\log(\Delta/\delta_{th})$ respectively. The selection of the appropriate fitting range is not always straightforward and results in a certain sensitivity of the results to this choice. It depends on the dynamic range (i.e. how many "quasi linear points" are available) dictated by the domain size (which limits the maximum filter or box size), the flame thickness (related to the inner cut-off scale) and the typical flame folding dictated by the integral length scales. In order to provide an idea

about the uncertainty we have changed the number of points of the existing curve fits from Fig. 2 by a reasonable amount. The resulting uncertainty was found to be smaller than 4.0% for the 2D analysis and 2.3% for the 3D data. The FD and BC methodologies showed comparable execution time and comparable sensitivity to input parameters in the analysis presented in this paper, while the evaluation of fractal dimension using the correlation dimension methodology is faster roughly a factor of 100 and requires considerably less memory.

It is worth noting that beside the fractal dimension the curve-fits in Fig. 2 yield the inner cut-off scale, which is in the case of the FD method the intersection of the solid line with the x-axis, whereas in case of the BC method, the x-coordinate of the intersection of the dotted and solid lines yields the inner cut-off scale. The evaluation of the CD inner cutoff scale follows the same philosophy as for the FD and BC methodology where the x -coordinate of the intersection of the dotted and solid lines yields the inner cut-off scale. Therefore, in the CD method, the intersection of the dotted line fitted at small scales and the solid line fitted at larger scales provides the measure of the inner cut-off scale. Figure 6 shows the inner cut-off scales normalised by δ_{th} for all methods for 2D and 3D. The results of the BC method in general yield somewhat smaller values compared to FD and CD. The present results suggest roughly a difference of the order of one thermal flame thickness between the cut-off scales (i.e., the inner cut-off scale for FD and CD are similar and on average δ_{th} larger than that obtained for BC). It can be seen from Fig. 6 that all methods yield comparable trends for the inner cut-off scale for the different flames and that the cut-off scale consistently decreases from case AP to EP, i.e., with increasing Karlovitz number. It is worth noting that the experimental analyses on 2D flame images by Cintosun et al. (2007) also reported quantitative differences in inner cut-off scale between different alternative methodologies.

5 Conclusions

The fractal dimensions of premixed turbulent flames have been evaluated using the filtering dimension method, the box-counting algorithm and the correlation dimension, using DNS databases of statistically planar (ranging from the wrinkled flamelets to the thin reaction zones regime) and Bunsen (representing wrinkled/corrugated flamelets regime) premixed flames. All methods provide results close to each other for benchmark problems. For the data analysed in this work, it has been found that the filtering dimension method tends to yield a fractal dimension larger than the box counting algorithm, which in turn gives larger values than the correlation dimension method. The maximum deviation of the fractal dimension for different methodologies over all cases including 2D and 3D analysis is about 7%. Nevertheless, for both 2D and 3D evaluations results are comparable to a large extent and show consistent trends for all cases. Further, the fractal dimension in 3D can be reasonably predicted by employing Mandelbrot's additive rule (i.e., $D_{3F} = D_{2F} + 1.0$) (Mandelbrot 1983) for a wide range of values of Damköhler and Karlovitz numbers irrespective of the methodology used for the evaluation of the fractal dimension. This suggests that the flame surface can roughly be represented by

an isotropic self-similar fractal surface for the parameter range considered here. Hence, either of these methodologies can be employed to extract the fractal dimensions of flame surfaces and Mandelbrot's additive rule can be utilised to obtain the true fractal dimension of the flame surface based on the fractal dimension extracted from 2D binarised experimental visualisations for a wide range of Damköhler and Karlovitz numbers. It has been also found that the inner cut-off scale determined from all three methods show a comparable behaviour and the same order of magnitude with smaller values for the BC method. The correlation dimension algorithm has considerably shorter run-times and provides physically consistent results. As it is based on infinitely thin flame surfaces, it does not suffer from the problem of flame self-interaction, observed for the FD method for highly wrinkled flames.

The present analysis is based on simple chemistry DNS data, but this simplification of chemistry is not expected to influence the conclusions of this analysis because the internal flame structure is not strictly relevant to this analysis because BC and CD methodologies are based on isosurfaces. Thus, the flame structure is often discarded for the postprocessing of the fractal dimension. Moreover, it has been demonstrated elsewhere (Keil et al. 2021a, b) that flame propagation and wrinkling statistics are qualitatively and to a large extent quantitatively very similar between detailed and simple chemistry simulations. Nevertheless, further analyses will be necessary for more complex configurations and detailed chemistry to extend and validate the findings of the current analysis.

Appendix

A straight line, the Koch Island and the Minkowski Island were used for validation in 2D, whereas a plane and a 3D type 1 quadratic Koch surface were used in 3D. The comparison between $D_F^{FD}, D_F^{BC}, D_F^{CD}$ and D_F^{Ha} for the aforementioned shapes is shown in Fig. 7, which shows a very good agreement between the results obtained by FD, BC, CD and the theoretically expected values. For cases F1–F5 the maximum errors with respect to the

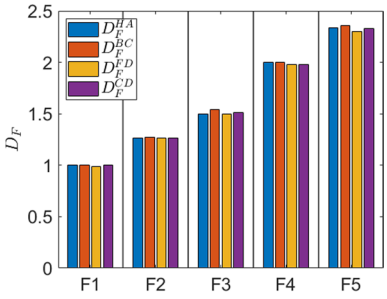

Fig. 7 The fractal dimensions according to the theoretical Hausdorff dimension D_F^{Ha}, the box-counting D_F^{BC}, the filtering dimension D_F^{FD} and the correlation dimension D_F^{CD} algorithm used here for a Line (F1), Koch curve (F2), Minkowski sausage (F3), Plane (F4) and 3D type 1 quadratic Koch surface (F5)

Hausdorff dimensions are 1.53, 0.07, 0.31, 1.05 and 1.43%, respectively. Similar deviations were reported by Chatakonda et al. (2013).

Acknowledgements The authors are grateful to EPSRC (Grant: EP/R029369/1) and ROCKET HPC facility for financial and computational support.

Author Contributions NC and MH conceptualised the analysis. MH performed the analysis, MH and MK prepared the figures, NC and MH wrote the original draft of the paper. NC and MK revised the paper. NC and MK supervised MH. All authors reviewed the manuscript.

Funding Open Access funding enabled and organized by Projekt DEAL.

Declarations

Conflict of interest The authors declare that they have no known competing financial interests or personal relationships that could have appeared to influence the work reported in this paper.

Ethical Approval This study does not involve any research with human participants and/or animals, so no ethical approval was required.

Informed Consent This study does not involve any research with human participants animals, so no informed consent was required.

References

Ahmed, U., Chakraborty, N., Klein, M.: Insights into the bending effect in premixed turbulent combustion using the flame surface density transport. Combust. Sci. Technol. **191**, 898–920 (2019a)

Ahmed, U., Klein, M., Chakraborty, N.: On the stress–strain alignment in premixed turbulent flames. Sci. Rep. **9**, 5092 (2019b)

Ahmed, U., Herbert, A., Chakraborty, N., Klein, M.: On the validity of Damköhler's second hypothesis in statistically planar turbulent premixed flames in the thin reaction zones regime. Proc. Combust. Inst. **38**, 3039–3047 (2021)

Bambauer, M., Hasslberger, J., Ozel-Erol, G., Chakraborty, N., Klein, M.: Surface topologies and self interactions in reactive and nonreactive Richtmyer–Meshkov instability. Sci. Rep. **13**, 837 (2023)

Boger, M., Veynante, D., Boughanem, H., Trouvé, A.: Direct Numerical Simulation analysis of flame surface density concept for large eddy simulation of turbulent premixed combustion. Proc. Combust. Inst. **27**, 917–925 (1998)

Bray, K.N.C.: Studies of the turbulent burning velocity. Proc. R. Soc. Lond. A **431**, 315–335 (1990)

Bray, K.N.C., Peters, N.: Laminar flamelets in turbulent flames. In: Libby, P.A., Williams, F.A. (eds.) Turbulent Reacting Flows, pp. 63–113. Academic Press Limited, London (1990)

Buczkowski, S., Kyriacos, S., Nekka, F., Cartilier, L.: The modified box-counting method: analysis of some characteristic parameters. Pattern Recogn. **31**, 411–418 (1998)

Candel, S.M., Poinsot, T.J.: Flame stretch and the balance equation for the flame area. Combust. Sci. Technol. **70**, 1–15 (1990)

Chaib, O., Zheng, Y., Hochgreb, S., Boxx, I.: Hybrid algorithm for the detection of turbulent flame fronts. Exp. Fluids **64**, 104 (2023)

Chakraborty, N.: Influence of thermal expansion on fluid dynamics of turbulent premixed combustion and its modelling implications. Flow Turb. Combust. **106**, 753–806 (2021)
Chakraborty, N., Klein, M.: A priori Direct Numerical Simulation assessment of algebraic flame surface density models for turbulent premixed flames in the context of large eddy simulation. Phys. Fluids **20**, 085108 (2008)
Chakraborty, N., Alwazzan, D., Klein, M., Cant, R.S.: On the validity of Damköhler's first hypothesis in turbulent Bunsen burner flames: a computational analysis. Proc. Combust. Inst. **37**, 2231–2239 (2019)
Charlette, F., Meneveau, C., Veynante, D.: A power-law flame wrinkling model for LES of premixed turbulent combustion Part I: non-dynamic formulation and initial tests. Combust. Flame **131**, 159–180 (2002)
Chatakonda, O.: Large Eddy simulations of premixed turbulent combustion. PhD thesis, University of New South Wales, Australia (2012)
Chatakonda, O., Hawkes, E.R., Aspden, A.J., Kerstein, A.R., Kolla, H., Chen, J.H.: On the fractal characteristics of low Damköhler number flames. Combust. Flame **160**, 2422–2433 (2013)
Cintosun, E., Smallwood, G.J., Gülder, Ö.L.: Flame surface fractal characteristics in premixed turbulent combustion at high turbulence intensities. AIAA J. **45**, 2785–2789 (2007)
Cohe, C., Halter, F., Chauveau, C., Gokalp, I., Gülder, O.: Fractal characterisation of high-pressure and hydrogen-enriched CH4–air turbulent premixed flames. Proc. Combust. Inst. **31**, 1345–1352 (2007)
Damköhler, G.: Der Einfluss der Turbulenz auf die Flammengeschwindigkeit in Gasgemischen. Zeitschrift für Elektrochemie und Angewante Physikalische Chemie **46**, 601–626 (1940)
Denet, B.: Possible roles of temporal in the bending of turbulent flame velocity. Combust. Theory Model. **3**, 585–589 (1999)
Driscoll, J.F.: Turbulent premixed combustion: flamelet structure and its effect on turbulent burning velocities. Prog. Energy Combust. Sci. **34**, 91–134 (2008)
Fureby, C.: A fractal flame wrinkling large eddy simulation model for premixed turbulent combustion. Proc. Combust. Inst. **30**, 593–601 (2005)
Gouldin, F.C., Bray, K.N.C., Chen, J.Y.: Chemical closure model for fractal flamelets. Combust. Flame **77**, 241–259 (1989)
Grassberger, P., Procaccia, I.: Measuring the strangeness of strange attractors. Phys. D **9**, 189–208 (1983)
Gülder, O., Smallwood, G.J.: Inner cutoff scale of flame surface wrinkling in turbulent premixed flames. Combust. Flame **103**, 107–114 (1995)
Keil, F.B., Amzehnhoff, M., Ahmed, U., Chakraborty, N., Klein, M.: Comparison of flame propagation statistics extracted from DNS based on simple and detailed chemistry Part 1: fundamental flame turbulence interaction. Energies **14**, 5548 (2021a)
Keil, F.B., Amzehnhoff, M., Ahmed, U., Chakraborty, N., Klein, M.: Comparison of flame propagation statistics based on DNS of simple and detailed chemistry. Part 2: influence of choice of reaction progress variable. Energies **14**, 5695 (2021b)
Keppeler, R., Pfitzner, M., Tay-Wo-Chong, L., Komarek, T., Polifke, W.: Including heat loss and quench effects in algebraic models for large eddy simulation of premixed combustion. In: Proceedings of ASME Turbo Expo 2012, GT2012–68689, Copenhagen, DK (2012)
Kerstein, A.: Fractal dimension of turbulent premixed flames. Combust. Sci. Technol. **60**, 441–445 (1988)
Klein, M., Sadiki, A., Janicka, J.: A digital filter based generation of inflow data for spatially developing direct numerical or large eddy simulations. J. Comp. Phys. **186**, 652–665 (2003)
Klein, M., Chakraborty, N., Ketterl, S.: A comparison of strategies for Direct Numerical Simulation of turbulence chemistry interaction in generic planar turbulent premixed flames. Flow Turb. Combust. **199**, 955–971 (2017)
Klein, M., Alwazzan, D., Chakraborty, N.: A Direct Numerical Simulation analysis of pressure variation in turbulent premixed Bunsen burner flames—Part 1: scalar gradient and strain rate statistics. Comput. Fluids **173**, 178–188 (2018)
Klein, M., Herbert, A., Kosaka, H., Böhm, B., Dreizler, A., Chakraborty, N., Papapostolou, V., Im, H.G., Hasslberger, J.: Evaluation of flame area based on detailed chemistry DNS of premixed turbulent hydrogen-air flames in different regimes of combustion. Flow Turb. Combust. **104**, 403–419 (2020)
Mandelbrot, B.B.: The Fractal Geometry of Nature. Freeman, New York (1983)
North, G.L., Santavicca, D.A.: The fractal nature of turbulent premixed flames. Combust. Sci. Technol. **72**, 215–232 (1990)
Peters, N.: Turbulent Combustion. Cambridge University Press (2000)
Poinsot, T., Lele, S.K.: Boundary conditions for direct simulation of compressible viscous flows. J. Comp. Phys. **101**, 104–129 (1992)
Pope, S.B.: The evolution of surfaces in turbulence. Int. J. Eng. Sci. **26**, 445–469 (1988)

Rasool, R., Chakraborty, N., Klein, M.: Algebraic flame surface density modelling of high pressure turbulent premixed bunsen flames. Flow Turb. Combust. 1–15 (2020)
Rasool, R., Chakraborty, N., Klein, M.: Effect of non-ambient pressure conditions and Lewis number variation on Direct Numerical Simulation of turbulent Bunsen flames at low turbulence intensity combustion and flame. Combust. Flame **231**, 111500 (2021)
Smallwood, G.J., Gülder, O., Snelling, D.R., Deschamps, B.M., Gokalp, I.: Characterization of flame front surfaces in turbulent premixed methane/air combustion. Combust. Flame **101**, 461–470 (1995)
Varma, A.R., Ahmed, U., Chakraborty, N., Klein, M.: Effects of turbulent length scale on the bending effect of turbulent burning velocity in premixed turbulent combustion. Combust. Flame **233**, 111569 (2021)
Wabel, T.M., Skiba, A.W., Driscoll, J.F.: Turbulent burning velocity measurements: extended to extreme levels of turbulence. Proc. Combust. Inst. **36**, 1801–1808 (2017)
Wang, R., Singh, A.K., Reddy Kolan, S., Tsotsas, E.: Fractal analysis of aggregates: correlation between the 2D and 3D box-counting fractal dimension and power law fractal dimension. Chaos Solut. Fractals **160**, 112246 (2022)
Yoshiyama, S., Tomita, E., Zhang, Z., Hemamoto, Y.: Measurement and simulation of turbulent flame propagation in a spark Ignition engine by using fractal burning model. SAE Trans. **110**, 2311–2323 (2001)
Yu, R., Lipatnikov, A.N.: DNS study of dependence of bulk consumption velocity in a constant-density reacting flow on turbulence and mixture characteristics. Phys. Fluids **29**, 065116 (2017)